CLM - P 26

This document is intended for publication in a journal, and is made available on the understanding that extracts or references will not be published prior to publication of the original, without the consent of the authors

CLM - P 26

United Kingdom Atomic Energy Authority

RESEARCH GROUP

Preprint

INFRA RED EMISSION FROM THE THETA PINCH

M. F. KIMMITT
G. B. F. NIBLETT

Culham Laboratory,

Culham, Abingdon, Berkshire

1963

UNCLASSIFIED
(Approved for Publication)

CLM - P 26

INFRA-RED EMISSION FROM THE THETA PINCH

by

M.F. Kimmitt*
G.B.F. Niblett

(Submitted for publication in Proceedings of the Physical Society)

ABSTRACT

Time-resolved measurements of infra-red emission from deuterium plasma in the theta pinch have been made at wavelengths between 70 and 250 microns using an indium antimonide photoconductive detector. At long wavelengths there is a sharp drop in emission near peak compression and this is attributed to increase of the critical plasma frequency beyond that corresponding to the wavelength of observation. Thus the effect affords a means of determining the electron density. For plasma whose dimensions and impurity content are known, the absolute measurement of the radiation at short wavelengths leads to an estimate of the electron temperature but as the emission depends only weakly on temperature the method is not of great precision.

Experimental values of density and temperature show reasonable agreement with those predicted by numerical solution of the one-dimensional two-fluid hydromagnetic equations, though the comparison suggests axial loss of plasma in the practical case. The measured electron temperature is in excess of 10^6 $^{\circ}$K for both trapped parallel and trapped reversed magnetic field. Bremsstrahlung from impurities makes an important contribution to the radiation from reversed field discharges and appropriate allowance for this increases the estimated temperature.

*Royal Radar Establishment, Malvern.

U.K.A.E.A. Research Group,
Culham Laboratory,
Nr. Abingdon,
Berks.

July, 1963

(C/18) IMG

C O N T E N T S

T A B L E S

1. INTRODUCTION

The recent development of fast photoconductive detectors sensitive at long wavelengths has made possible time-resolved measurements of continuous bremsstrahlung radiation from fully-ionized plasmas in the far infra-red. The first measurements of this type, made on the ZETA plasma (Harding and Roberts 1961), used a detector sensitive over the range 0.1 - 2.0 mm to provide measurements of electron concentration in the range 10^{14} to 10^{15} electrons/cm^3 and electron temperatures in the neighbourhood of 10^5 ^{o}K. Under these conditions, and given the large dimensions of ZETA, it was possible to observe the transition from an optically thin plasma to one with a black body spectrum.

The present paper is concerned with the extension of this technique to study plasma generated by rapid magnetic compression in the theta pinch. High powered theta pinch experiments utilize compression times of the order of microseconds to produce plasmas with diameters of about a centimetre, densities between 10^{16} and 10^{17} electrons/cm^3, and temperatures from 10^6 to 10^7 ^{o}K (Gabriel et al 1962). These conditions are convenient for studying the emission spectrum of the plasma in the neighbourhood of the plasma wavelength. A detailed knowledge of the shape and intensity of the spectrum in this region offers in principle a method of estimating both the electron density and the electron temperature. The major aim of the experiment was to examine this possibility.

2. INFRA-RED RADIATION FROM A PLASMA

The intensity of bremsstrahlung radiation per unit wave number from a plasma one centimetre thick is given by, [Allen 1963],

$$j_{\frac{1}{\lambda}} = \frac{B\ g\ n_e\ n_i\ Z^2\ \exp(-hc/k\ T_e\ \lambda)}{(k\ T_e)^{\frac{1}{2}}}\ \text{erg sec}^{-1}\ \text{cm}^{-3}\ \text{steradian}^{-1}\ \text{cm} \quad \ldots(1)$$

This expression assumes a Maxwellian distribution of electron velocities corresponding to a temperature T_e. The electron and ion particle densities are represented by n_e and n_i, Z is the ionic charge, g is the Gaunt factor and the other symbols have their usual meaning. B is a constant given by $\frac{16}{3}\left(\frac{\pi}{6m_e^3}\right)^{\frac{1}{2}} \frac{e^6}{c^2}$ whose numerical value is 1.91×10^{-36}. At wavelengths such that $\lambda \gg \frac{hc}{kT_e}$ the Gaunt factor [Gaunt, 1930] may be written as

$$g = \frac{\sqrt{3}}{\pi} \ln\left(\frac{3}{2}\frac{kT_e}{hc}\lambda\right) \qquad \ldots(2)$$

so that for 10^6 °K g varies from about 5 at 100 microns wavelength to 6 at 500 microns. In addition the exponential term in equation (1) is equal to unity so that apart from the small variation in g the bremsstrahlung intensity is constant as the wavenumber varies.

At long wavelengths the effects of self-absorption and stimulated emission become important and these can be incorporated in equation (1) by taking its product with the factor $\frac{1 - e^{-K\ell}}{K}$ where the absorption coefficient K is given by

$$K = \frac{B}{2c}\, g\, n_e\, n_i\, Z^2 \frac{\lambda^2}{(kT_e)^{\frac{3}{2}}} \quad (\mathrm{cm}^{-1}) \qquad \ldots(3)$$

and the thickness ℓ of the plasma is taken as one centimetre. The effect of this term is to convert the expression for volume emission to the usual formula for the Rayleigh-Jeans region of the black body spectrum,

$$j_{\frac{1}{\lambda}} = \frac{2ckT}{\lambda^2} \text{ erg sec}^{-1} \text{ cm}^{-2} \text{ steradian}^{-1} \text{ cm} \qquad \ldots(4)$$

In Fig.1 the above relationships are plotted for electron concentrations of 10^{16} and 10^{17} cm^{-3} and an electron temperature of 10^6 °K.

Also included in Fig.1 is the plasma wavelength λ_p defined as $\lambda_p = (\pi m_e c^2/n_e e^2)^{\frac{1}{2}}$. Since this is the free space wavelength corresponding to the frequency of plasma oscillations it is convenient to refer to it in terms of plasma resonance, and to the spectrum in this region as the plasma resonance spectrum. The free-free emission on the long wavelength side of λ_p is indicated in Fig.1 by a dotted line in order to emphasise that no account has been taken of plasma resonance effects in computing the curves. The graph illustrates clearly the suitability of the theta pinch for studying the spectrum in the neighbourhood of λ_p. The high temperatures and small plasma dimensions move the black body curve to the left of the graph, i.e. towards long wavelengths, whereas the high densities shift the plasma wavelength in the opposite direction. As a result the plasma resonance wavelength is well separated from the black body regime.

For wavelengths greater than λ_p the refractive index of the plasma is

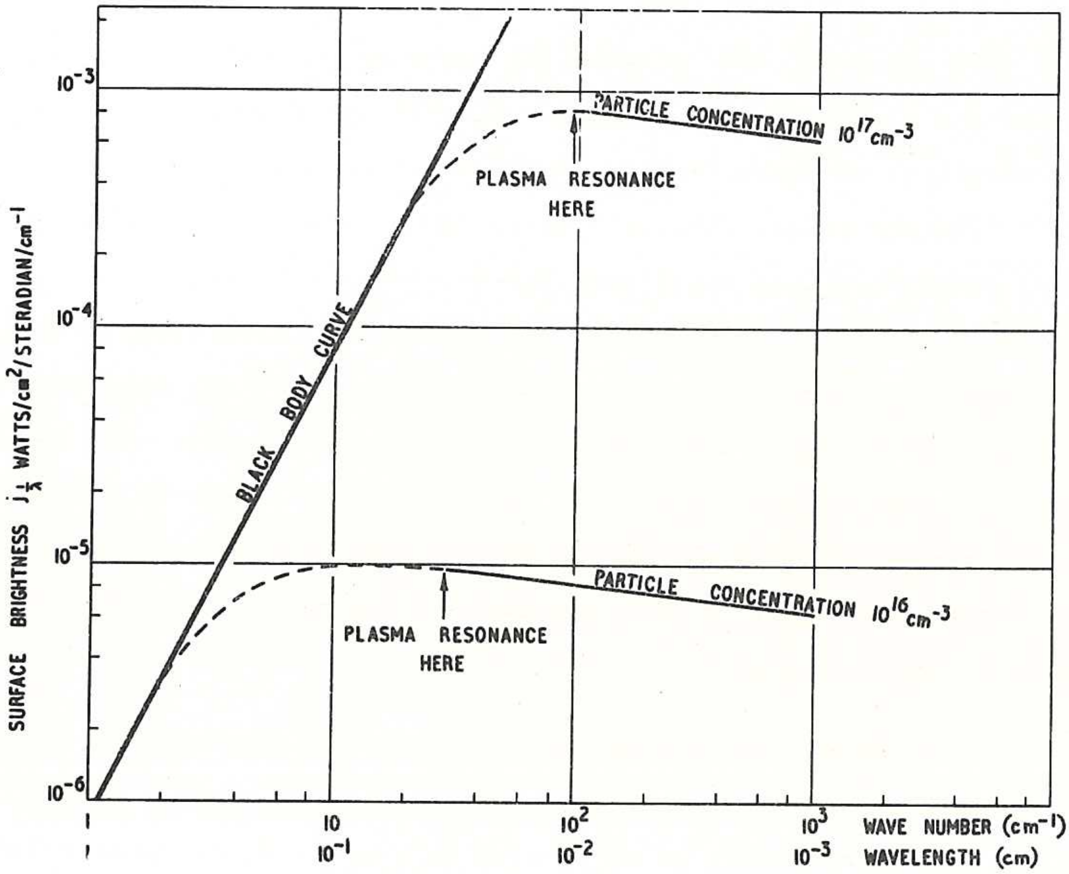

CLM- P26 Fig. 1 Surface brightness as a function of wavelength for a pure deuterium plasma at a temperature of 10^6 °K and particle concentrations 10^{16} and 10^{17} cm^{-3}. The plasma is taken as one centimetre thick.

almost purely imaginary so that incident waves are largely reflected. Applying Kirchhoff's law, the plasma is therefore expected to be a poor emitter of such radiation. The experiments described below confirm this expectation since a sharp drop in emitted radiation is observed as we pass from the short to the long wavelength side of plasma resonance.

3. EXPERIMENTAL METHOD

The theta discharge was produced by applying to initially unionized deuterium gas a rapidly varying axial magnetic field generated by switching a a low inductance condenser bank on to a single-turn coil of length 40 cm and internal diameter 10 cm. The coil encircled an alumina discharge tube of internal diameter 8.2 cm containing the deuterium. These dimensions were chosen so as to give a peak density low enough for the plasma wavelength to fall within the range of the infra-red detector. Thus the densities and temperatures produced in the experiment are not the highest that can be reached with present equipment. The condenser bank consisted of 100 μF capacity charged to 30 kV and gave a half-period of 5.8 μs with a peak field on the second half-cycle of 45 kilogauss. A diagram of the coil and tube assembly is shown in Fig.2.

It is well known that plasma conditions at peak compression in the theta pinch depend on the sign and strength of the initial trapped magnetic field. By making all measurements on the second half-cycle the trapped field could be varied by adjusting the starting gas pressure. As the pressure was increased over the narrow range from 48 mTorr to 53 mTorr the trapped field varied from being parallel to the external field to being anti-parallel or reversed. Infra-red spectra were recorded for three experimental regimes:
(a) trapped parallel field, corresponding to a starting pressure of 48 mTorr;
(b) minimal (i.e. near zero) trapped field, corresponding to 50 mTorr;
(c) trapped reversed field at a starting pressure of 53 mTorr. Reproducibility of these conditions was monitored by an external magnetic probe placed between the single turn coil and the discharge tube; this provided characteristic waveforms identifying the regimes defined above.

The far infra-red emission was measured using a spectrometer and indium antimonide detector. The spectrometer, which has been described fully

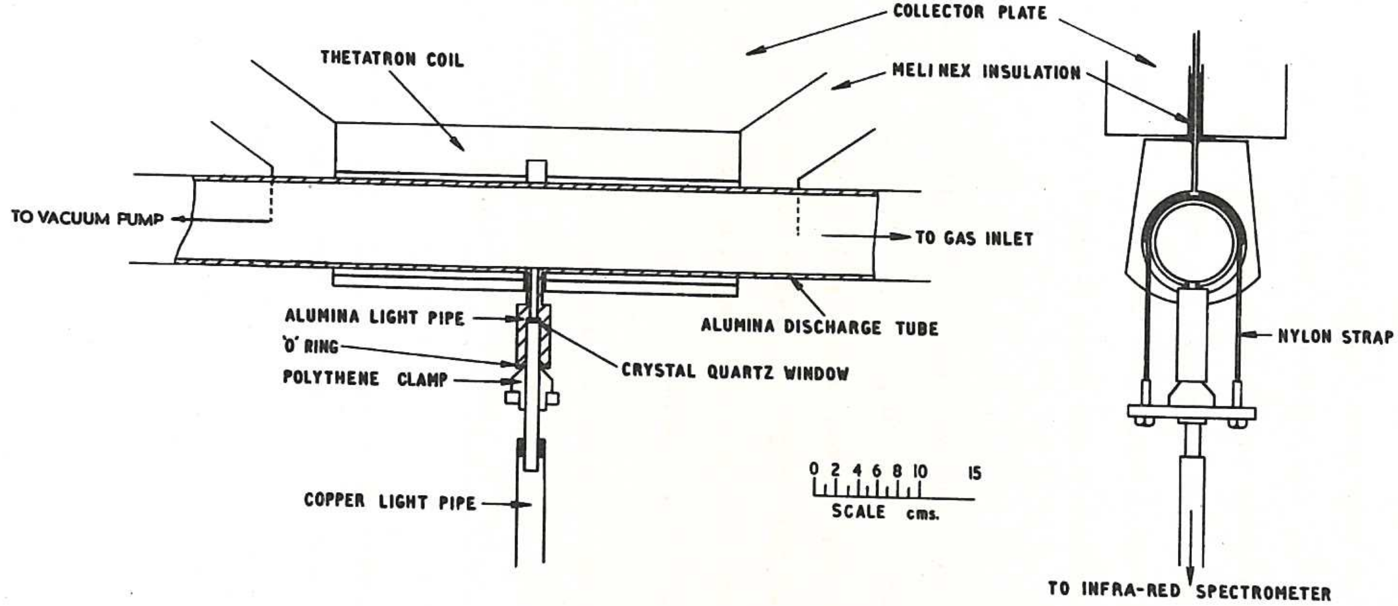

CLM - P 26 Fig. 2 Coil assembly for infra - red experiment.

elsewhere (Harding et al 1961), was an evacuated instrument employing a blazed grating ruled with alternative spacings of 0.5 or 0.25 mm and it passed a bandwidth between 5 and 10% of the designated wavelength. The detector was a modified version of the high purity indium antimonide photo-conductor (Putley 1960) employed in previous far infra-red experiments. The modification consists in operating the detector in a magnetic field of between 7 and 25 kilogauss supplied by a superconducting niobium-zirconium solenoid. Used this way the detector is tunable between 250 and 60 microns by adjusting the magnitude of the magnetic field. At the operating temperature of 4.2 ^{o}K the spectral response is sufficient to render the detector insensitive to unwanted orders from the diffraction grating. A fuller description of the detector has been given by Brown and Kimmitt (Brown and Kimmitt 1963).

Measurement of the time-variation of infra-red emission was made at ten selected wavelengths in the range 70 to 250 microns and in each case the detector output was amplified, displayed on an oscilloscope and photographed. The response time of the complete system was 0.3 μs. All measurements were made in the mid-plane of the coil, and the method of inserting a copper light pipe through the coil and discharge tube is shown in detail in Fig.2.

A high speed image converter camera manufactured by Space Technology Laboratories Inc. was used to take streak photographs of the plasma. The camera was aligned with its slit in the horizontal plane defined by the light pipe and the feed-plates to the coil. In this way the diameter of the plasma and its distance from the light pipe could be measured throughout the half-cycle. It should be noted that the light guide entered the discharge tube at a point opposite the electrical feed plates. Due to non-uniformities in the magnetic field the plasma drifted across the tube during the half-cycle; nevertheless it remained strictly in the horizontal plane viewed by the light pipe.

The oscilloscope signals were converted to absolute values of surface brightness by calibration of the spectrometer and detector system. This was done by mounting a mercury discharge lamp of the approximate dimensions of the plasma at the centre of the discharge tube opposite the light pipe and measuring the signal at the specified wavelengths under conditions identical to those of the main experiment. The emission of the mercury lamp in the far infra-red was known by calibration against a source of measured temperature and emissivity. The accuracy of this calibration is estimated as ± 10%.

To complete the conversion to surface brightness it was necessary in addition to assign a thickness to the plasma. Assuming the plasma to have a uniform density equal to its peak value, an 'effective' diameter was calculated so as to give a total bremsstrahlung emission equal to that from a plasma whose diameter is given by the streak photographs and whose radial density distribution is provided by the numerical calculations described below. The effective diameter calculated this way was about 1 cm compared with a measured value of 1.5 cm and will be in error by no more than 20%. If anything the effective diameter has been minimised to ensure that the quoted plasma temperatures are an underestimate.

4. EXPERIMENTAL RESULTS

A representative streak photograph showing the plasma motion during the second half-cycle is shown in Fig.3. The plasma implodes radially during the first 0.3 μs then oscillates at high frequency as the field increases and finally expands to the wall. During this process it remains in the horizontal plane defined by the camera slit but drifts gradually away from the light pipe so that by peak compression the centre of the plasma has moved about 2 cm from the axis of the tube. It is important to note that light coming from the walls originates beyond the ends of the coil; underneath the coil itself no wall light can be seen. This supports the assumption that the light pipe is receiving infra-red radiation directly from the plasma.

Oscillograms of the infra-red emission from a discharge with zero trapped field are shown in Fig.4 at wavelengths of 85, 140, 150 and 225 microns. The intensity rises in the early stages but then decreases at about 0.3 μs. This initial rise and fall is particularly clear in records (b),(c) and (d) and is a consequence of the variation in solid angle presented by the plasma to the light pipe during the implosion phase. The subsequent rapid oscillations are not discernible since the time-response of the detector is long compared with their period. After the implosion,

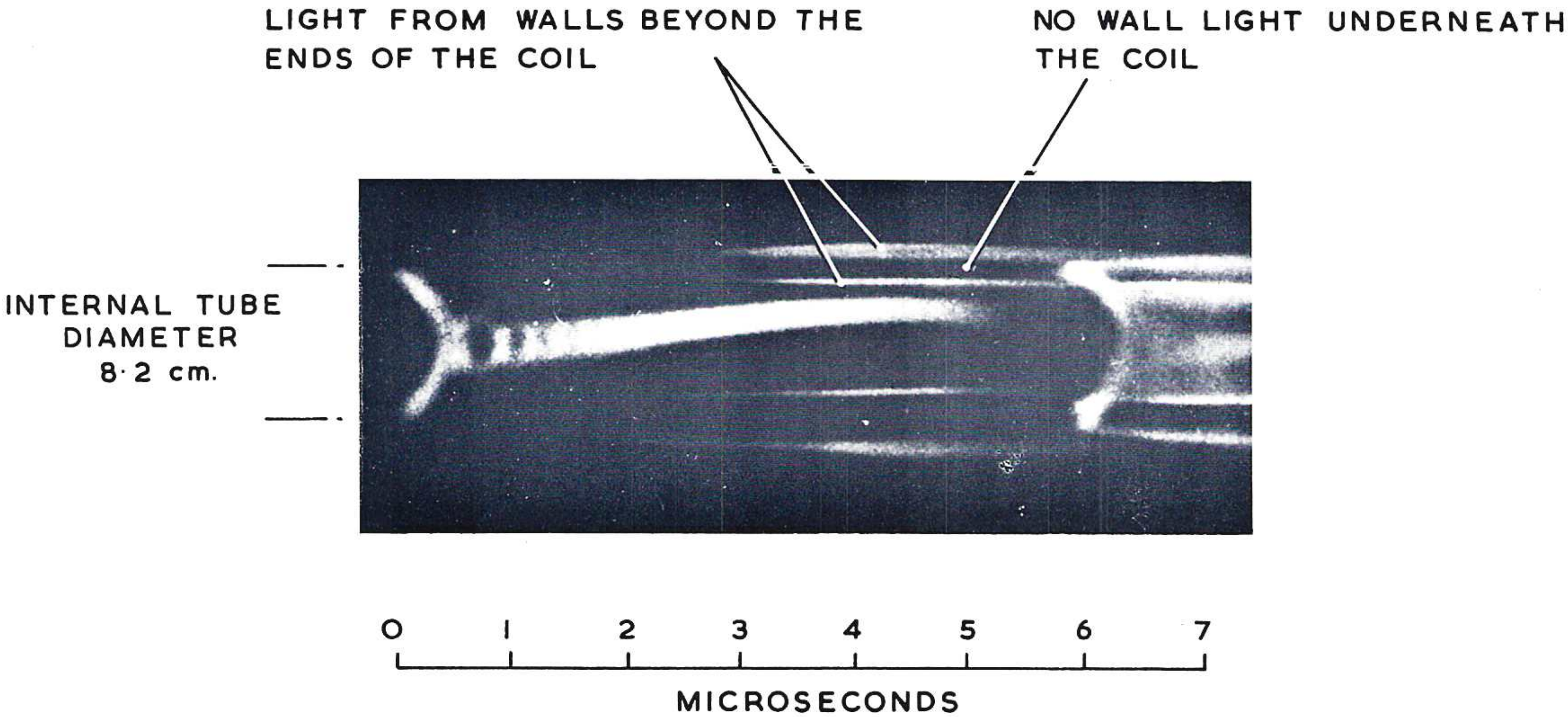

CLM - P 26 Fig. 3 Streak photograph of deuterium discharge during second current half-cycle.

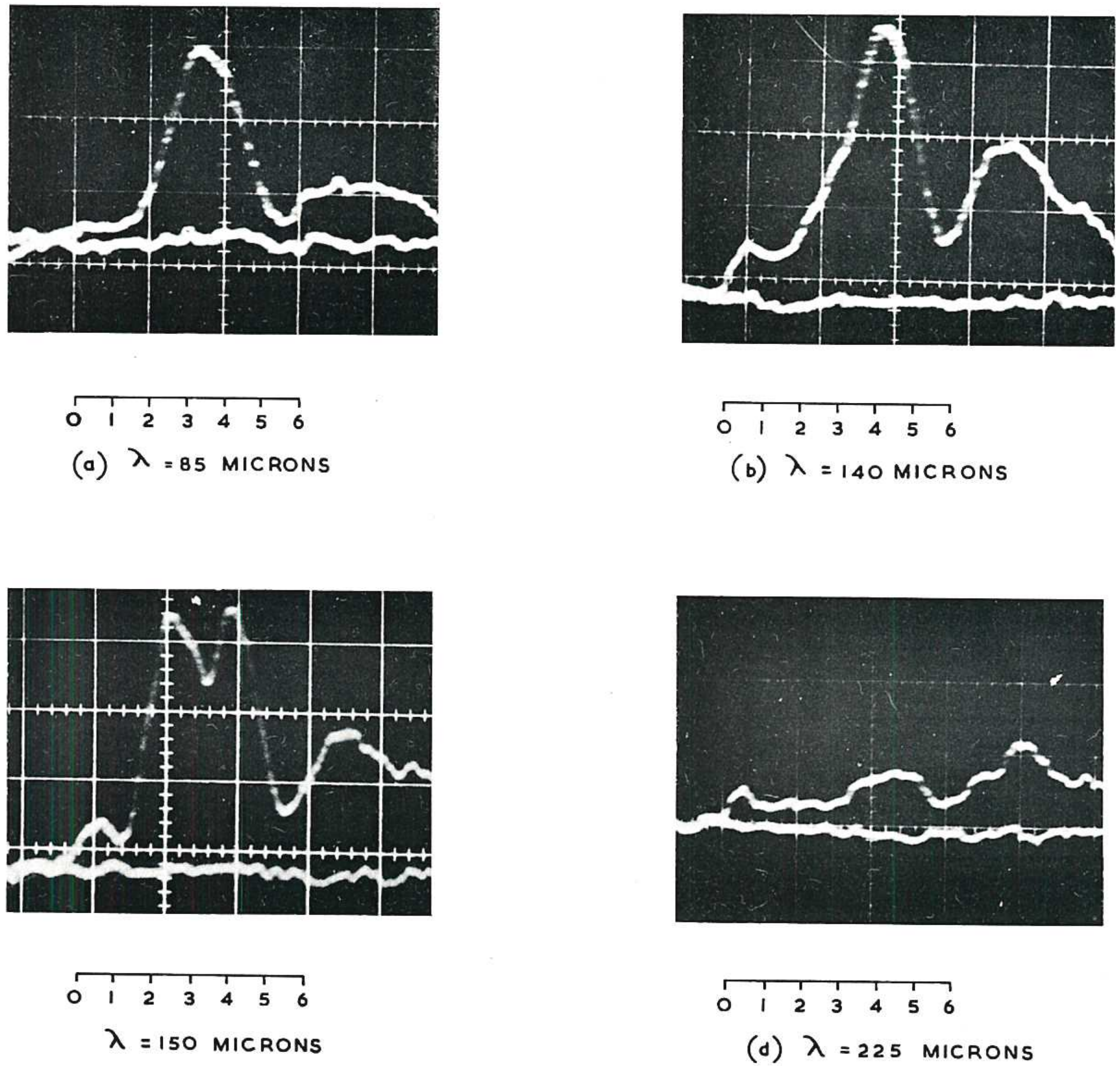

CLM-P 26 Fig. 4 Infra-red emission as a function of time for wavelengths of 85, 140, 150 and 225 microns. All the waveforms were taken under conditions of minimal trapped field. Time is measured in microseconds from the beginning of the second half-cycle.

the infra-red emission increases uniformly and records (a) and (b) show a continuous increase to a peak value followed by a steady decline. However, beyond 140 microns there is a significant change in the nature of the emission. At 150 microns the emission falls sharply just before peak compression and rises again just afterwards. We attribute this fall to plasma resonance i.e. the plasma density increases beyond that corresponding to a plasma wavelength of 150 microns. The emission at 225 microns is much less strong since plasma resonance sets in soon after the end of the implosion.

Because of the relatively long time response of the detector the analysis of the oscillograms has been confined to peak compression. In Fig.5 the measured surface brightness is plotted as a function of wave number for the reversed field regime, and the range over which plasma resonance is observed is recorded in the figure. Similar graphs were plotted for the other plasma regimes. The peak electron concentration is determined from the oscillograms by noting the shortest wavelength at which the plasma resonance effect is observed: the electron density corresponding to this wavelength is the value required. The estimated electron densities are presented in Table I which shows a maximum value of 5×10^{16} cm^{-3} for the minimal trapped field condition.

Fig. 5 shows that the radiant intensity at short wavelengths is approximately constant as expected. The measured value of $j_{\frac{1}{\lambda}}$ in this region can be combined with the deduced electron density to give a rough estimate of electron temperature, and Table I shows the results of this calculation for a pure deuterium plasma. For all three regimes the calculated temperature is greater than 10^6 ^oK which is in agreement with estimates based on soft X-ray measurements.

As the wavelength increases the emission falls off sharply long before the normal absorption processes become significant. At wave-lengths of 175 microns and beyond (in Fig.5) the curve has a black body slope with an absolute magnitude appropriate to a temperature of only 10^4 ^oK. Thus the import of the measurements is that at wavelengths greater than the plasma wavelength the spectrum approximates to that of a black body with a temperature about a hundred times lower than the true kinetic temperature of the electrons. A more detailed investigation of the spectrum under these conditions

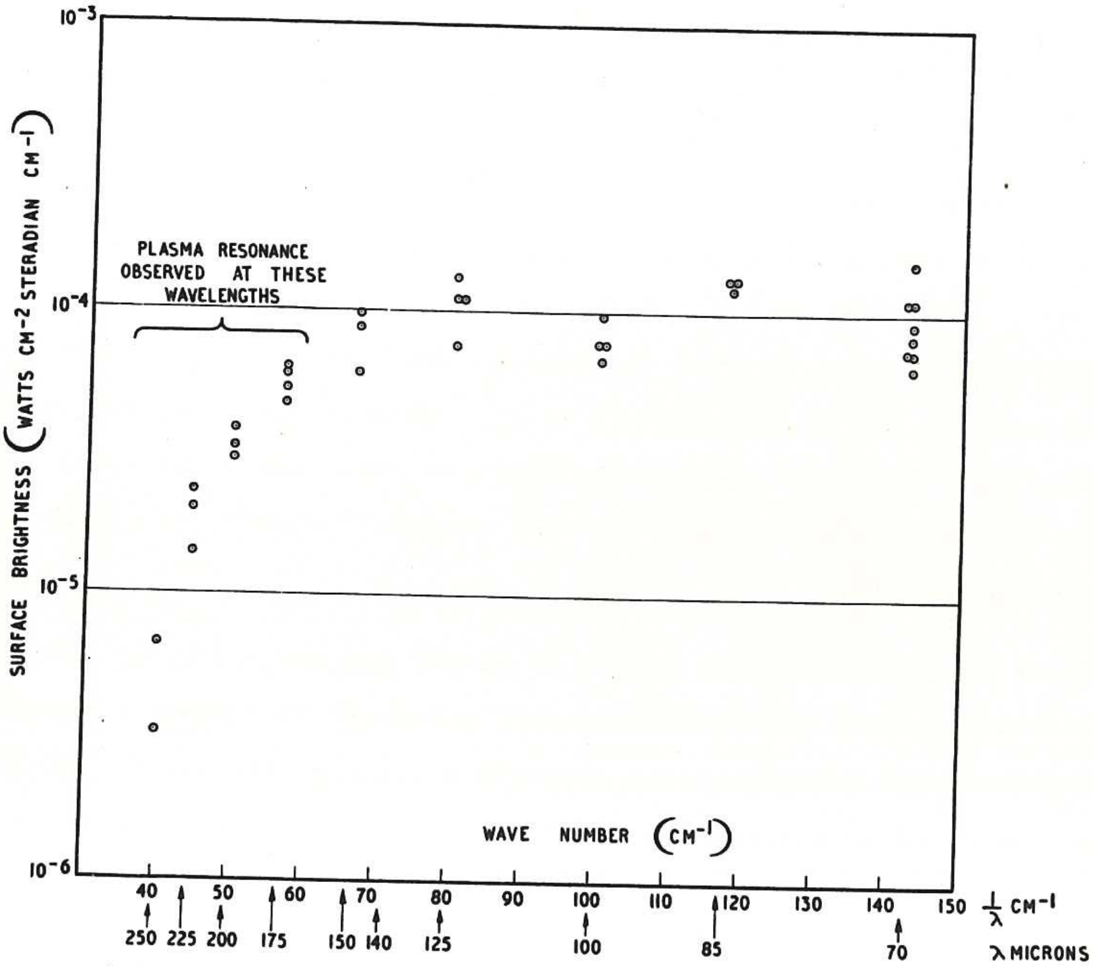

CLM - P 26 Fig. 5 Infra-red spectrum of THETATRON plasma. Surface brightness at peak compression as a function of wavelength (trapped reversed field).

is thus clearly necessary. At wavelengths near to but greater than λ_p the emission will presumably be determined by the width of the plasma boundary. At still longer wavelengths, when electron-ion collisions contribute to the plasma refractivity, the spectrum should coincide with the black body curve at the true plasma temperature.

5. DISCUSSION

Here we assess the likely errors of these estimates of plasma density and temperature. Since n_e is inversely proportional to λ_p^2, a variation of 10% in λ_p corresponds to 20% in n_e so that at best the density measurements can be no more precise than this. The estimate of temperature is much less reliable for it depends on high powers of quantities that are known only imprecisely. From equation (1) it follows that for a given radiant intensity, T_e is proportional to n_e^4 so that in terms of wavelength, which is the measured quantity, T_e is proportional to λ_p^8. An uncertainty of 10% in judgment of λ_p leads therefore to an uncertainty of more than a factor of two in temperature. Hence the quoted values must be regarded only as a rough guide to electron temperature.

Table I includes numerical values of n_e and T_e provided by Mr. D.L. Fisher who solved numerically the one-dimensional two-fluid hydromagnetic equations for the theta pinch using the coil dimensions and magnetic field employed in the experiment and specifying a starting deuterium pressure of 50 mTorr. The values of initial trapped field correspond to those of the three experimental regimes. A detailed account of this numerical technique applied to the theta pinch has been published previously (Niblett and Fisher 1962). At peak compression the measured density is lower by a factor of two than that predicted numerically and we attribute this discrepancy to axial loss of plasma from the coil. A similar conclusion was reached by Fünfer and his colleagues (Fünfer et al, 1962) in an experiment using an optical interferometer to measure plasma density. Though Table I shows a discrepancy in terms of absolute densities both theory and experiment agree in assigning the highest density to the zero field regime.

The theoretical and experimental values of electron temperature are in satisfactory agreement save for the discharge with trapped reversed field where the predicted figure is four times greater than that given by the infra-red measurement. Here we should remark that most of the corrections applicable to the measured value would increase it. For example the bremsstrahlung intensity is proportional to $T_e^{-\frac{1}{2}}$ so that the cooler regions of the plasma radiate most strongly. In addition we have probably underestimated the effective plasma diameter and this would result in a low value for electron temperature.

If no allowance be made for bremsstrahlung radiation from plasma impurities the measured temperature would be too low and we attribute the divergence between theory and experiment mainly to this source. Absolute radiation measurements in the visible (Gabriel et al. 1962) have shown that in reversed field discharges the plasma contains about 1% of oxygen impurity atoms which at high temperatures are fully stripped to give an ionic charge of eight. A small fractional degree of impurity atoms x (where $x \ll 1$) leads to a modification of equation (1) which then becomes:

$$j_{\frac{1}{\lambda}} = \frac{B\ g\ n_e^2 \exp(-hc/k\ T_e\ \lambda)}{(k\ T_e)^{\frac{1}{2}}} \quad [1 + x\ Z(Z-1)] \qquad \ldots(5)$$

For 1 or 2% of oxygen atoms with $Z = 8$ this leads to an increase in estimated temperature by a factor of between two and five which is sufficient to remove the variance between theory and experiment. The source of the greater impurity of reversed field discharges is probably to be found in the strong contact with the wall at the end of the first half cycle when the magnetic field changes sign.

6. CONCLUSIONS

The measurement of far infra-red radiation from a fast theta pinch in deuterium has shown clear evidence of a fall-off in emission at wavelengths longer than the plasma wavelength and has led to an estimate of peak electron concentration of 5×10^{16} cm^{-3} with an uncertainty of about 20%. A value for electron temperature has been obtained from the absolute size of the infra-red signal at short wavelengths but the experimental error is high - about a factor of two. For all three plasma regimes the estimated temperature is greater than 10^6 $^{\circ}$K so that the infra-red technique shows agreement with previous soft X-ray measurements. This agreement is of importance because of the widely variant electron energies (separated by six orders of magnitude) on which the two methods depend.

Agreement with numerical solution of the one-dimensional hydromagnetic equations is reasonably satisfactory but axial loss of plasma is indicated. Temperatures in reversed field discharges are lower than the predicted values but this is consistent with the greater impurity of the reversed field discharge and the figures are reconciled by an impurity content of just over 1%. At wavelengths greater than the plasma wavelength the emission spectrum makes an approximate fit to a black body curve, but at a temperature about two orders of magnitude lower than the kinetic temperature of the electrons.

7. ACKNOWLEDGEMENTS

We wish to express our thanks to Messrs. N.R. Gilbert, G.E.S. Harding and P. Porteous who assisted with the experiments, and to Dr. T.S. Green who collaborated in an earlier series of measurements. Mr. D.L. Fisher was responsible for the numerical solution of the hydromagnetic equations and kindly provided the data included in Table I.

REFERENCES

ALLEN, C.W. Astrophysical Quantities. University of London Press. 1963.

BROWN, M.A.C.S. and KIMMIT, M.F. Brit. Commun. Electron. To be published. 1963.

FÜNFER, E. et al. Z. Naturf., vol.17a, p.967, 1963.

GABRIEL, A.H., et al. J. Quant. Spectrosc. Radiat. Transfer, vol.2, p.491, 1962.

GAUNT, J.A. Phil. Trans. Roy. Soc., vol.229, p.163, 1930.

HARDING, G.N. et al. Proc. Phys. Soc., vol.77, p.1069, 1961.

HARDING, G.N. and ROBERTS, V. Salzburg Conference on Controlled Nuclear Fusion Research. 1961.

NIBLETT, G.B.F. and FISHER, D.L. Culham Laboratory Report CLM - R 19, 1962.

PUTLEY, E.H. Proc. Phys. Soc., vol.76, p.802, 1960.

TABLE I

EXPERIMENTAL AND NUMERICAL ESTIMATES OF ELECTRON DENSITY AND TEMPERATURE AT PEAK COMPRESSION

	Experimental Results			Numerical Results		
Discharge Regime	Measured Surface Brightness at Peak Compression watts/cm^2/Steradian/cm^{-1}	Peak Electron Concentration cm^{-3}	Electron Temperature ^oK	Initial Trapped Field Kilogauss	Peak Electron Concentration cm^{-3}	Electron Temperature ^oK
Parallel Trapped Field	4.4×10^{-5}	2.8×10^{16}	1.9×10^6	+ 2.0	7×10^{16}	2.3×10^6
Minimal Trapped Field	1.25×10^{-4}	5.0×10^{16}	2.3×10^6	- 0.2	1.0×10^{17}	2.8×10^6
Reversed Trapped Field	9.8×10^{-5}	3.7×10^{16}	1.1×10^6	- 2.0	7×10^{16}	5.1×10^6